

COVER PAGE

Document downloaded by @DAEL

Sat Nov 21 15:19:09 2026
For personal use

When automatic English translation is provided, only the original document is authentic.
The EAA cannot be held responsible of any translation error

Bibliographical reference

Experimental Demonstration of the Modification of the Resonances of a Simplified Self-Sustained Wind Instrument Through Modal Active Control, Thibaut Meurisse, Adrien Mamou-Mani, Simon Benacchio, Baptiste Chomette, Victor Finel, David B. Sharp and René Caussé, Acta Acustica **vol. 101** (Number 3), 2015, pp. 581-593

DOI
https://doi.org/10.3813/AAA.918854

Acta Acustica united with Acustica
Vol. 101 (2015) 581 – 593

DOI 10.3813/AAA.918854

Experimental Demonstration of the Modification of the Resonances of a Simplified Self-Sustained Wind Instrument Through Modal Active Control

Thibaut Meurisse[1)], Adrien Mamou-Mani[1)], Simon Benacchio[1)], Baptiste Chomette[2)], Victor Finel[2)], David B. Sharp[3)], René Caussé[1)]

[1)] UMR STMS IRCAM - CNRS - UPMC - 1 place Igor Stravinsky, 75004 Paris, France.
meurisse.thibaut@gmail.com

[2)] Sorbonne Universités, UPMC Université Paris 06, CNRS, UMR 7190 Institut Jean Le Rond d'Alembert, 75005 Paris, France

[3)] Acoustics Research Group, Faculty of Maths Computing and Technology, DDEM, MCT, The Open University, Walton Hall, Milton Keynes, MK7 6AA, Bucks, Great Britain

Summary

This paper reports the experimental results of modifying the resonances of wind instruments using modal active control. Resonances of a simplified bass clarinet without holes (a cylindrical tube coupled to a bass clarinet mouthpiece including a reed) are adjusted either in frequency or in damping in order to modify its playing properties (pitch, strength of the harmonics of the sound, transient behaviour). This is achieved using a control setup consisting of a co-located loudspeaker and microphone linked to a computer with data acquisition capabilities. Software on the computer implements an observer (which contains a model of the system) and a controller. Measuring and adjusting the transfer function between the speaker and microphone of the control setup enables modifications of the input impedance and the radiated sound of the instrument.

PACS no. 43.50.Ki, 43.75.Ki

1. Introduction

This study aims at modifying the resonances of the air column of a musical wind instrument using modal active control [1].

Musical wind instruments, such as the clarinet which can be modeled as an excitation coupled to a resonator via a non-linear coupling [2, 5, 7, 6, 3, 4] (see Figure 1), are self-sustained oscillating systems. Over the past few decades, classical active control (which uses gains, phase shifting, filters and delays) has been applied to musical instruments. It was first applied to percussion and string instruments [8, 9, 10], but has also been applied to wind instruments. In particular, classical active control has been used to play a complete octave on a flute with no holes [11]. To achieve this, the incident wave was absorbed by a speaker at the end of the tube, and replaced by a chosen reflected wave. The classical approach has also been used to modify the resonance of a trombone mute [12] and all the resonances of a simplified clarinet with gain and phase shifting [13]. In this last case, the control could not modify the modes separately.

Received 29 July 2014,
accepted 26 January 2015.

Modal active control of a self-sustained system can be achieved using a control setup consisting of a co-located microphone and speaker linked to a computer with data acquisition capabilities. The co-location ensures that the system is more robust [1, 10]. That is, the efficiency of the control (i.e. stability and performance) is relatively unaffected by external changes (temperature, time, etc.). Software on the computer implements a *controller* and an *observer*, which uses a modal state-space representation of the system. This is a mathematical model which represents the system in terms of state variables (expressed as vectors and matrices) containing the modal parameters (frequency, damping) of the system. Modal active control enables the modal parameters to be modified so that individual resonances can be adjusted to reach target frequency and damping values [14, 15]. Simulations have shown that the control of a self-sustained oscillating system such as a clarinet is theoretically feasible [16]. There have been relatively few applications of modal active control to musical instruments [17, 18] and no application to wind instruments to the authors' knowledge.

The relative values of the frequencies and damping factors of the acoustic resonances of a musical instrument have a major role in determining both the pitch and timbre of the played note [19]. However, the exact relationship between resonance modal parameters (frequency and

© S. Hirzel Verlag · EAA

Document downloaded by @DAEL, 2026-11-21 15:19:12 - personal use only

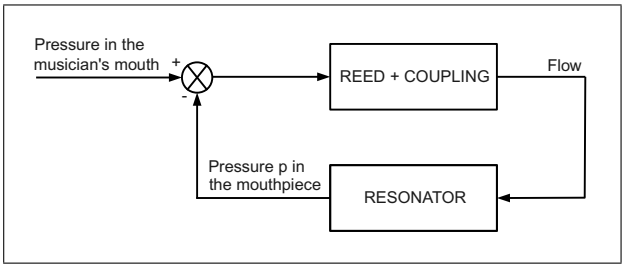


Figure 1. Model of a self-sustained wind instrument [3].

damping) and the instrument intonation and playability remains a subject of investigation [20, 21]. Modal active control provides a tool to study this relationship experimentally. It also enables the role of each resonance in maintaining the self-sustained oscillations in playing conditions to be explored.

In this paper, experimental results resulting from applying modal active control to a simplified bass clarinet (a cylindrical tube coupled to a bass clarinet mouthpiece with a reed) are presented. The control is used with the intent of adjusting the resonances of the instrument, thereby altering the timbre of the sound it produces as well as its playing properties and input impedance. Such adjustments provide similar effects to those that would result from modifying the instrument's bore profile [22, 23], as the input impedance of an instrument is determined by its internal geometry [19].

In Section 2, the state-space representation of the resonator of the simplified instrument (i.e. a cylindrical tube) used by the observer of the control setup is presented. The principle of the modal control is then explained. In Section 3, the controlled simplified bass clarinet with embedded co-located microphone and speaker is described. By measuring and adjusting the transfer function between the speaker and microphone of the control setup, modifications of the input impedance and radiated sound of the instrument are achieved. Examples of the control of a single resonance in both frequency and damping are presented, as well as examples of the control of several resonances simultaneously, in order to demonstrate the possibilities offered by the control.

2. Modal State-Space Model

In this section, the modal state-space representation of the resonator of the simplified wind instrument is presented. This representation takes into account the excitation from the speaker of the control setup, as well as the monitoring of the pressure by the microphone of the control setup. Finally, the designs of the observer and controller elements of the control setup are described.

2.1. The Resonator

Modal active control makes it possible to control the frequencies and damping factors of the modes of a system. To be able to apply modal active control, however, the system must be expressed in terms of a state-space model, comprising vectors and matrices which describe the system's dynamics. Here, a modal state-space model of the resonator of the simplified bass clarinet is described.

The state-space model of the cylindrical tube used in this paper is derived in [14] and can be found with more details in [16]. The diameter of the tube is sufficiently small compared with its length L_t, that the tube can be considered to be a one-dimensional waveguide with spatial coordinate z, where $0 \leq z \leq L_t$. In the model, the speaker element of the control setup is positioned at $z = z_s$ and the microphone at $z = z_m$. The microphone and speaker are co-located ($z_s = z_m$).

The pressure in the tube, with the speaker incorporated in the tube wall, is described by the nonhomogeneous equation [14]

$$\frac{1}{c^2}\ddot{p}(z,t) = p''(z,t) + \rho_0 \dot{v}_s(t)\delta(z - z_s), \tag{1}$$

where p is the acoustic pressure, v_s the speaker baffle velocity, ρ_0 the density of the acoustic medium and δ the Kronecker delta. The $''$ symbol represents the second order spatial derivative and the $\dot{}$ and $\ddot{}$ symbols represent respectively the first and second order time derivatives. $\rho_0 \dot{v}_s$ represents the command sent by the control speaker.

Assuming that $p(z,t)$ can be projected on a modal base, and using separation of variables, the pressure can be written as

$$p(z,t) = \sum_{i=0}^{\infty} V_i(z) q_i(t), \tag{2}$$

where V_i is the modal shape of mode i (the spatial domain function of $p(z,t)$) and q_i the modal displacement of mode i (the temporal domain function of $p(z,t)$) inside the tube. To obtain a modal state-space description of the cylindrical tube, with embedded control setup, truncated with r modes and including a proportional modal damping, let

$$\mathbf{x}(t) = \begin{bmatrix} q_i(t) \\ \dot{q}_i(t) \end{bmatrix}, \quad i = \{1 \ldots r\}, \tag{3}$$

where $\mathbf{x}(t)$ is the state vector used in the linear model so that the system can be described as

$$\begin{cases} \dot{\mathbf{x}}(t) = \mathbf{A}\mathbf{x}(t) + \mathbf{B}u_s(t), \\ y(t) = \mathbf{C}\mathbf{x}(t), \end{cases} \tag{4}$$

where $u_s(t)$ is the signal produced by the controller (referred to as the command in the context of active control) and transmitted to the speaker, $y(t)$ is the output of the system, and

$$\mathbf{A} = \begin{bmatrix} \mathbf{0}_{r,r} & \mathbf{I}_{r,r} \\ -\mathrm{diag}(\omega_i^2) & -\mathrm{diag}(2\xi_i\omega_i) \end{bmatrix}, \quad i = \{1 \ldots r\} \tag{5}$$

is the dynamical matrix which contains the frequencies ω_i and damping factors ξ_i of the resonances of the cylindrical tube for the i_{th} mode. The modal parameters of these modes are extracted from a transfer function measured between the microphone and speaker of the control

Document downloaded by @DAEL, 2026-11-21 15:19:12 - personal use only

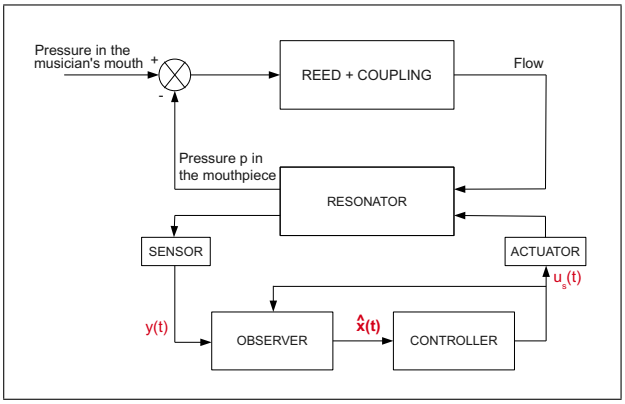


Figure 2. Model of a self-sustained wind instrument [3] with control setup. $y(t)$ is defined in Equation (4), $u_s(t)$ is defined in Equation (8), and $\hat{\mathbf{x}}(t)$ is defined in Equation (10).

setup with a Rational Fraction Polynomials (RFP) algorithm [24].

Meanwhile, $\mathbf{I}_{r,r}$ is the identity matrix, and

$$\mathbf{B} = \begin{bmatrix} \mathbf{0}_{r,1} \\ K_{s_1} K_{m_1} V_1^2(z_s) \\ \vdots \\ K_{s_r} K_{m_r} V_r^2(z_s) \end{bmatrix} \tag{6}$$

is the actuator matrix, where the transfer functions of the speaker (K_{s_i}) and microphone (K_{m_i}) are assumed to be pure gains, where $V_i(z)$ is as described in Equation (2), and where $K_{s_i} K_{m_i} V_i^2(z)$ is identified between the speaker and the microphone with the RFP algorithm. Finally,

$$\mathbf{C} = \begin{bmatrix} \mathbf{1}_{1,r} & \mathbf{0}_{1,r} \end{bmatrix} \tag{7}$$

is the sensor matrix.

2.2. Modal Control

Schematically, a self-sustained wind instrument is a reed coupled to a resonator (cylindrical tube) through a non linear coupling (see Figure 1). To apply modal active control to this resonator to modify its frequencies and damping factors, a control setup (consisting of a co-located microphone and speaker linked by a Luenberger [25] observer and a controller) is added to the resonator (see Figure 2). The observer directly receives the signal measured by the microphone; its role is to rebuild the state vector $\mathbf{x}(t)$ using a model of the system and the measurement $y(t) = p(t)$. Let $\hat{\mathbf{x}}(t)$ be the built state vector estimated by the Luenberger observer. $\hat{\mathbf{x}}(t)$ is used by the controller to generate a command $u_s(t)$ that is transmitted through the speaker in order to apply the control to the resonator. This command $u_s(t)$, which appears in Equation (4), can be expressed as

$$u_s(t) = -\mathbf{K}\hat{\mathbf{x}}(t), \tag{8}$$

where $\mathbf{K}$ is the control gain vector used to move the conjugate poles s_i of the $\mathbf{A}$ matrix (i.e. its eigenvalues) so that [26]

$$\begin{aligned} Re(s_i) &= -\xi_i \omega_i, \\ Im(s_i) &= \pm\omega_i \sqrt{1-\xi_i^2}. \end{aligned} \tag{9}$$

$\mathbf{K}$ is determined, together with the $\mathbf{A}$ and $\mathbf{B}$ matrices, using a pole placement algorithm (in this work, the algorithm developed by Kautsky et al. [27] is used).

By using control gains $\mathbf{K}$, these poles can be moved in order to reach new, target values for the resonator's frequencies (angular frequencies ω_{i_t}) and damping factors (ξ_{i_t}). These new poles are the eigenvalues of $(\mathbf{A} - \mathbf{BK})$.

The dynamics of the observer used to estimate the state of the system can be written

$$\begin{cases} \dot{\hat{\mathbf{x}}}(t) = \mathbf{A}\hat{\mathbf{x}}(t) + \mathbf{B}u_s(t) + \mathbf{L}\big(y(t) - \hat{y}(t)\big), \\ \hat{y}(t) = \mathbf{C}\hat{\mathbf{x}}(t) \end{cases} \tag{10}$$

where $\mathbf{L}$ is the observer gain vector. $\mathbf{L}$ is chosen such that the error between the state and its estimation, $e_{\mathbf{x}}(t) = \mathbf{x}(t) - \hat{\mathbf{x}}(t)$, converges to zero. This error can also be expressed as [1]

$$\dot{e}_{\mathbf{x}}(t) = (\mathbf{A} - \mathbf{LC}) e_{\mathbf{x}}(t). \tag{11}$$

The eigenvalues of the observer are the eigenvalues of (**A** - **LC**). They may be chosen without regard to those of the controlled system. However, the observer needs to be quicker than the controller for the control system (observer + controller) to work and stay stable. To achieve this, the real part of its eigenvalues must be at least 2 times more negative than those of the controlled system (the instrument). In order not to degrade the precision of the observer, these real parts are chosen between 2 and 6 times more negative. $\mathbf{L}$ is calculated, along with the $\mathbf{A}$ and $\mathbf{C}$ matrices, using the same pole placement algorithm as used when determining $\mathbf{K}$.

Details of the simplified bass clarinet, together with a number of experimental measurements, are presented and discussed over the remainder of the paper.

3. Measurements

In this section, the simplified wind instrument with incorporated control setup is presented. Examples of the effect of the control on the transfer function between the speaker and microphone of the control setup are provided. The resulting effect on the input impedance, which is representative of the interaction between the musician and the instrument, and on the sound produced by the instrument are observed. The sound is measured one meter away from the output of the instrument. Three sets of examples of the possibilities of the control are presented, with increasing complexity. First, only one resonance (here, the seventh) is controlled in terms of both frequency and damping factor. Next the control is made more complex and aims at adjusting the damping of many resonances (here, seven resonances, from resonance 4 to resonance 10). Finally, the control is applied with the aim of modifying both the frequencies and damping factors of seven resonances in such a way that they become harmonically related to the first input impedance peak of the tube, without altering the amplitudes of the impedance peaks (here, resonances 3 to 9 are controlled). The sounds used in this section may be

Document downloaded by @DAEL, 2026-11-21 15:19:12 - personal use only



Figure 3. Top: Simplified bass clarinet (a cylindrical tube with a bass clarinet mouthpiece and a reed) with embedded control setup with co-located microphone and speaker. Top right corner: control setup removed from the instrument. Bottom: Schematic view of the instrument with embedded control setup. The left red arrow indicates the position 5 cm from the open end of the tube, while the right red arrow indicated the position 9 cm from the mouthpiece.

found at http://instrum.ircam.fr/?p=647. Section 3.5 characterises the differences obtained on the radiated sounds using three criteria, the sound level, the spectral centroid and the pitch.

3.1. The Instrument

The simplified instrument with incorporated control setup is shown in Figure 3. The instrument comprises a closed-open cylindrical tube of length 1.19 m and radius 11 mm coupled to a bass clarinet mouthpiece and reed. The control setup consists of a co-located speaker and microphone and is placed 50 mm from the open end of the tube. The speaker is linked to the tube by a cylindrical cavity of length 5 mm and radius 20 mm and a hole of mean thickness 1.5 mm and radius 5 mm. The components used in the control setup are a 2″ Tymphany Peerless PLS-P830983 speaker and an Endevco piezoelectric pressure resistive model 8507C-5 microphone. The control is achieved using Simulink under Xenomai [28, 29, 30], a real-time development framework cooperating with the Linux kernel, which allows a latency of about 20 μs when controlling 10 modes.

To choose the optimum position for the speaker and the microphone, the input impedance of the instrument is measured (i) without speaker and microphone, (ii) with the speaker and the microphone located 9 cm from the mouthpiece and (iii) with the speaker and the microphone located 5 cm from the open end of the tube (see arrows on Figure 3). These input impedances, measured using the BIAS system with an equivalent volume of the mouthpiece, are on Figure 4. During these particular measurements, there is no control applied. Up to 800 Hz, the speaker and the microphone located close to the open end of the tube do not have a big effect on the input impedance, but there is an increase of the frequency of the resonances higher than the sixth. With the speaker and the microphone located close to the mouthpiece, the frequency of the first resonance is modified (from 71 Hz to 59 Hz) and its amplitude is reduced by 8 dB. Moreover, the second and third resonances have wide reduction of amplitude (22 dB and 10 dB respectively), and modifications either in amplitude

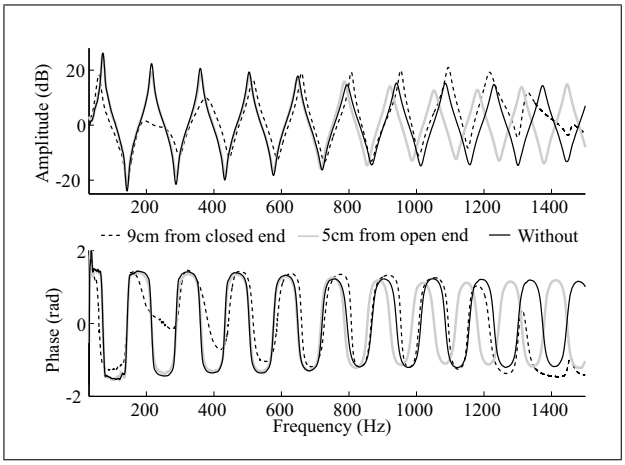


Figure 4. Top: Input impedance of a closed-open cylindrical tube with length 1.19 m and radius 11 mm without speaker and microphone (solid black line), with the speaker and the microphone located 9 cm from its closed end (dash black line) and with the speaker and the microphone located 5 cm from its open end (solid gray line). Bottom: Phases of the input impedances of a closed-open cylindrical tube without speaker and microphone (solid black line), with the speaker and the microphone located 9 cm from its closed end (dash black line) and with the speaker and the microphone located 5 cm from its open end (solid gray line). No control is applied for these measurements.

and frequency are observed for all the other resonances. When blowing in the tube through the mouthpiece, it becomes impossible to produce a sound with the speaker and the microphone located close to the mouthpiece, but it is still possible to produce a sound when they are located close to the open end of the tube. These problems with the speaker and the microphone located near the mouthpiece may come from the cavity and speaker added, as the amplitude of the modes is maximum at this place, then the perturbations are greater. It has been then chosen to place the speaker and the microphone close to the open end of the tube, so that the perturbations of the tube resonances are minimum.

Figure 5 shows the transfer function measured between the microphone and the speaker of the control setup, and the transfer function identified using a RFP algorithm. The identified transfer function is a sum of ten identified modes, from the second mode to the eleventh. As an example, identified modes 6 and 7 are shown on Figure 5. Table I gives the modal parameters of the identified modes, where $b_i = K_{s_i} K_{m_i} V_i^2(z_s)$ are the components of matrix **B** in Equation (6). The first mode of the tube (71 Hz) is not identified. This is mainly due to the position of the control setup, close to the open end of the tube, where the first modes are low in amplitude. It is also due to the resonance frequency of the speaker (147.5 Hz) below which its response is very weak. The second mode is not well identified, particularly with regard to its phase, with a difference of 0.62 rad (0.2 π). The 9 other modes are well identified. The acoustical resonance frequency of the control setup is approximatively 1500 Hz. As a result, measurements have been limited to frequencies below this

Document downloaded by @DAEL, 2026-11-21 15:19:12 - personal use only

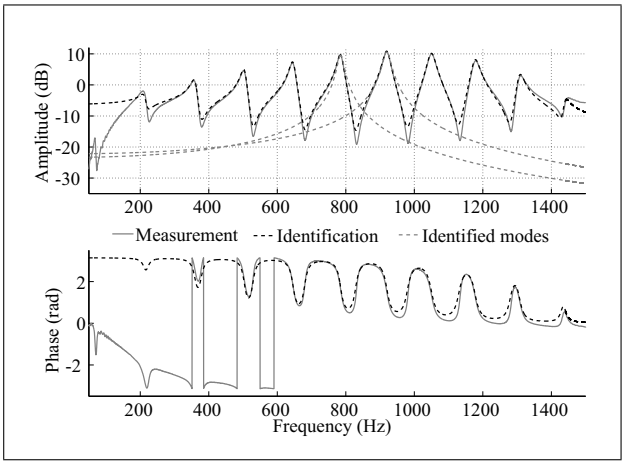


Figure 5. Top: Measured (solid gray line) and identified (dash black line) transfer functions of the tube, and identified modes 6 and 7 (dash gray lines). Bottom: Measured (solid gray line) and identified (dash black line) phase of the transfer functions of the tube.

Table I. Modal parameters of the identified modes.

Resonance	Frequency (Hz)	Damping	b_i
2	214	0.0448	-1514
3	361	0.0262	-4096
4	504	0.0172	-6750
5	646	0.0141	-10505
6	785	0.0114	-16753
7	920	0.0113	-23519
8	1050	0.0115	-28429
9	1177	0.0100	-25423
10	1306	0.0083	-14126
11	1439	0.0065	-1971

value. Figure 6 shows the poles of the identified modes (blue circles). Note that the modes transverse to the tube are not modeled. First, their frequencies are much higher than 1500 Hz (the first mode has a frequency of 8994 Hz, see Appendix). Moreover, no problem related to spillover [1] were encountered during this study. However, a study of the effect of the control on the first transversal mode is reported in the Appendix.

3.2. Control of the frequency and damping of the seventh resonance

In this section, 2 cases of control of the seventh resonance of the system are studied:

- case **1**: decrease of the frequency, from 920 Hz to 860 Hz, with no modification of the damping factor,
- case **2**: damping factor reduced by a factor of 4, with no modification of the frequency.

Figure 6 shows the pole placement for these two cases.

Figure 7 shows the transfer functions of the system, measured between the speaker and the microphone of the control setup, without control and in the two cases of control.

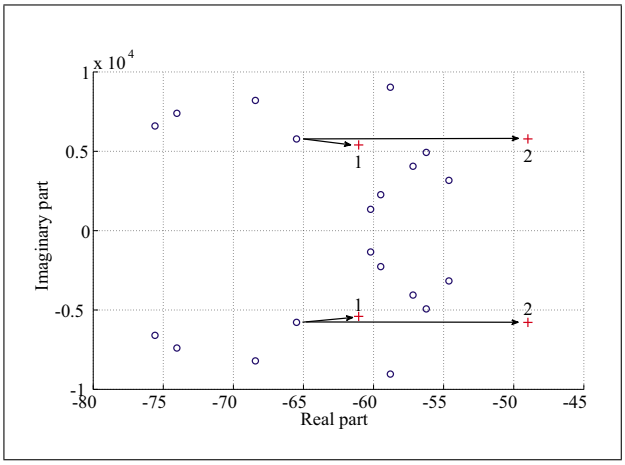


Figure 6. Pole placement for the pole of the seventh resonance in cases **1** and **2**. Only poles 2 to 11 are shown.

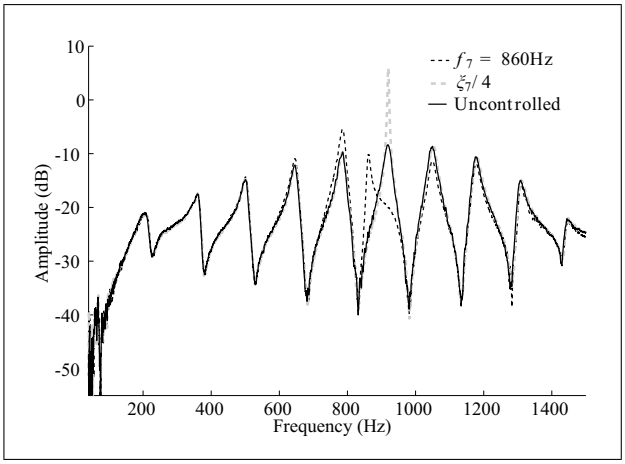


Figure 7. Transfer functions of the tube without control (solid black line) and with two cases of control of the seventh resonance; **1** : decrease of the frequency from 920 Hz to 860 Hz (dash black line), **2**: damping factor reduced by a factor of 4, (dash light gray line).

The effects of the controls on the seventh peak are detailed in Table II. The frequency of the peak is close to the targeted frequency for the seventh resonance in case **1**. However, moving the frequency of the peak has also resulted in a reduction in its amplitude and its damping factor is decreased. The damping factor of the peak is close to the targeted damping factor for the seventh resonance in case **2**. Altering the damping of the seventh resonance results in modifications of its amplitude. It is increased when the damping is decreased.

Effects on the other peaks are also observed when controlling the seventh resonance. In case **1**, the amplitudes of peaks 5, 6, 8 and 9 are affected, particularly peak 6 which increases by 4 dB. This may be due to the contribution of the seventh mode in its low frequencies side. Case **2** shows very little modifications on the other peaks (less than 1 dB or 3 Hz).

Figure 8 shows comparisons between measurements and simulations in control cases **1** and **2**. In the simula-

Document downloaded by @DAEL, 2026-11-21 15:19:12 - personal use only

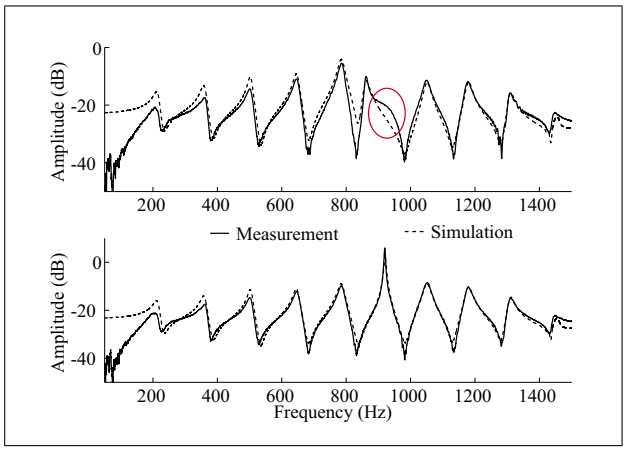


Figure 8. Top: Measured (solid black line) and simulated (dash black line) transfer function of the tube with control case **1** applied. The circle shows the hill in the high frequency side of the measured seventh resonance. Bottom: Measured (solid black line) and simulated (dash black line) transfer function of the tube with control case **2** applied.

Table II. Modal parameters (frequency, amplitude, damping) of the seventh resonance of the transfer functions (Figure 7) in the uncontrolled case (U) and in cases **1** ($f_7 = 860$ Hz), and **2** (ξ_7 reduced by a factor of 4), differences between targeted and obtained frequency and damping in cases **1** and **2**, and modifications obtained on the amplitude between the uncontrolled and controlled cases.

Case	U	1	2
Frequency (Hz)	920	862	920
Target (Hz)	NA	860	920
Differences (cents)	NA	3	0
Damping	0.0113	0.0065	0.0025
Target	NA	0.0113	0.0028
Differences (%)	NA	44	11
Amplitude (dB)	-8.4	-10.2	6
Modifications (dB)	NA	-1.8	+14.4

tions, the instrument is described by the model developed in Section 2, with **A**, **B** and **C** identified experimentally in Section 3.1 (see Table I). The model used by the observer and the instrument are then identical. In both cases, the behaviour of the controlled resonance is very close between simulation and measurement. At low frequency there are differences in both cases, mainly regarding to the amplitude of the peaks. In case **1**, there is a hill in the high frequency side of the measured seventh resonance (circled in Figure 8), which does not appear in the simulation. This is due to modeling errors, mainly as the speaker resonance has not been used in the model, but also as the first resonance is not modeled and as the second resonance is not well identified. These errors do not affect the control and the system remains stable.

Figure 9 shows the input impedance magnitude of the system without control and in the two cases of control. The effects of the controls on the seventh peak are detailed

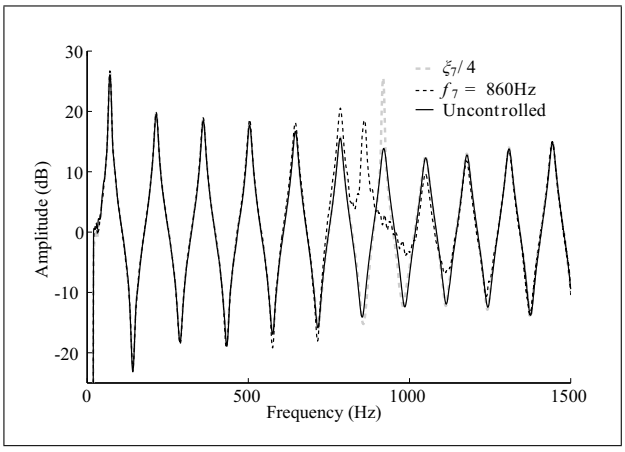


Figure 9. Input impedance magnitude of the tube without control (solid black line) and with two cases of control of the seventh resonance; **1**: decrease of the frequency from 920 Hz to 860 Hz (dash black line), **2**: damping factor reduced by a factor of 4, (dash light gray line).

Table III. Frequency and amplitude of the seventh peak of the input impedance (Figure 9) in the uncontrolled case (U) and in cases 1 and 2, differences between attempted and obtained frequency in cases 1 and 2, and modifications obtained on the amplitude between the uncontrolled and controlled cases.

Case	U	1	2
Frequency (Hz)	920	860	919
Differences (cents)	NA	0	1
Amplitude (dB)	13.9	18.5	25.6
Modifications (dB)	NA	+4.6	+11.7

in Table III. The frequency of the peak is exactly that targeted for the seventh resonance in case **1**. The control of the frequency of the seventh resonance has also resulted in its amplitude being increased. In case **1**, the antiresonances after peaks 6, 7, 8 and 9 are increased in amplitude by 20 dB to 5 dB, so that the antiresonances between peaks 6 and 7 and between peaks 7 and 8 almost disappear. Altering the damping of the seventh resonance results in modifications of the amplitude of the related peak in the input impedance. It is increased when the damping is decreased. There are also little modifications of the frequency in case **2**.

Effects on the other peaks are also observed when controlling the seventh resonance frequency. In case **1**, the amplitudes of peaks 5, 6, 8 and 9 are affected, particularly peak 6 which increases by 5 dB. Case **2** shows very little modifications of the other peaks, as for the transfer function.

Figure 10 shows the spectrogram of the sound emitted by the instrument, when blowing in it, with the control case **1** applied ($f_7 = 860$ Hz). In this figure, the control is applied between times 2 and 5 seconds. The control is applied while blowing in order to avoid reproductivity problems. With and without control, the pitch of the instrument corresponds to the first resonance of the tube.

Document downloaded by @DAEL, 2026-11-21 15:19:12 - personal use only

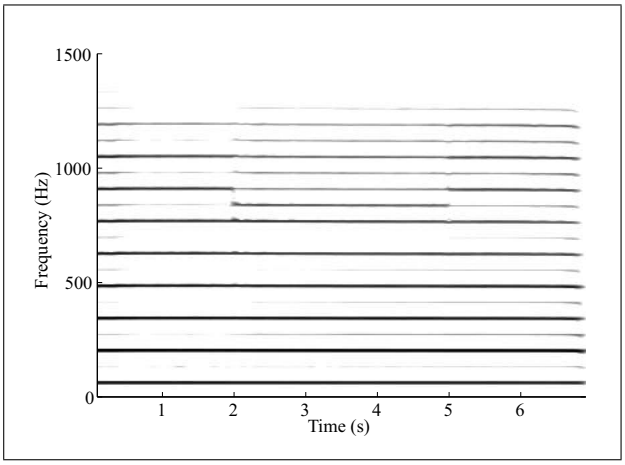


Figure 10. Spectrogram of the sound emitted by the instrument in case **1**. The control is applied for 3 seconds, between time 2 and 5 seconds.

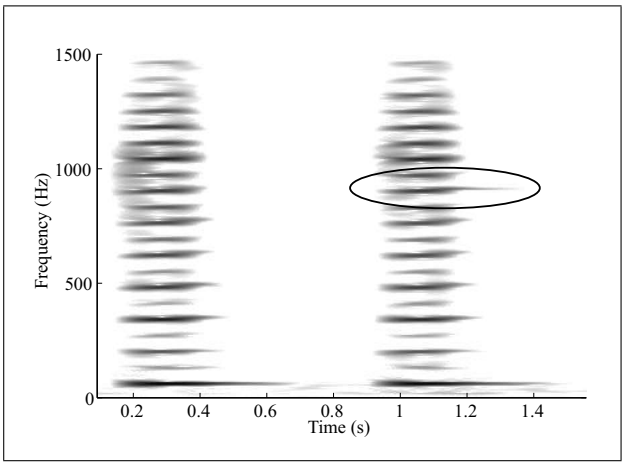


Figure 11. Spectrogram of the sound emitted by the instrument in case **2** while producing two short sounds. The first one is done without control, the second with the control applied. The seventh harmonic is circled black for the second sound.

When the control is not applied, the sound shows only the odd harmonics, which is characteristic of a closed-open tube. When the control is applied, the amplitude of the seventh odd harmonic (about 920 Hz) is weakened, because the seventh resonance is less harmonically related to the fundamental. Indeed, the resonances of a closed-open cylinder have frequencies so that $f_n = (2n-1)f_1$. The more the frequency of a resonance is far from these values, the less it is harmonically related to the fundamental. Here, as the frequency is moved from $f_7 = 920\,Hz$ to $f_7 = 860\,Hz$, it is far from the theoretical value of $f_7 = (2\times 7-1)f_1 = 923\,Hz$, with $f_1 = 71\,Hz$. However, the even harmonics 6 to 9 (i.e. the harmonics with frequencies of $6\times 2\times f_1$ to $9\times 2\times f_1$, about 852 Hz, 994 Hz, 1136 Hz and 1278 Hz) are enhanced, particularly the sixth even harmonic which is really close to the frequency of the controlled seventh resonance. This correlates with what has been observed on Figure 9. When the control stops, the sound is again composed mainly of the odd harmonics of the fundamental. This control case is referred to as case **1** in Table IX.

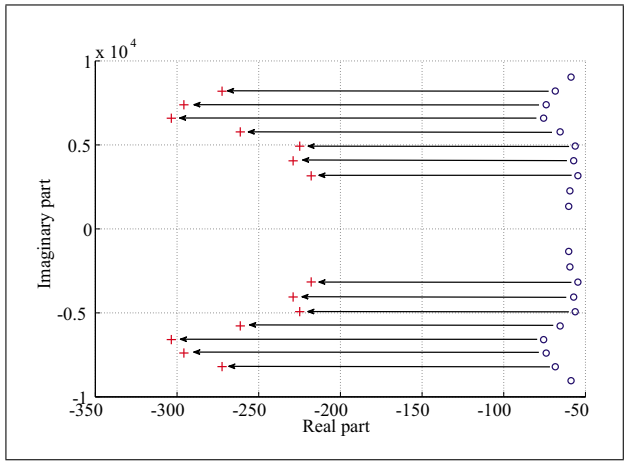


Figure 12. Pole placement for the pole of resonances 4 to 10 when increasing their damping factors by a factor of 4. Only poles 2 to 11 are shown.

In control case **2** (ξ_7 reduced by a factor of 4), applying the control while blowing continuously in the tube does not have noticeable effects. Figure 11 shows two short sounds (*slaps*), the first without the control applied, and the second with the control applied. Each time, the sound is produced while blowing in the tube for 0.25 seconds approximatively. When the control is not applied, only the fundamental is still present when the blow stops, for 0.25 seconds. With the control applied, the fundamental has the same behaviour as without control, and a sound close to the seventh harmonic (circled black in Figure 11) is still present when the blow stops, for 0.2 seconds. This sound corresponds to the frequency of the seventh resonance of the tube (920 Hz), which is not exactly harmonically related with the fundamental of the sound (the seventh harmonic has a frequency of 910 Hz). This is why it cannot be heard while blowing continuously.

3.3. Control of the damping of resonances 4 to 10

In Section 3.2, the control of only one resonance has been explored. In this section, the control of the damping factors of the resonances 4 to 10 is studied.

Figure 12 shows the pole placement when the damping factors of the resonances 4 to 10 is increased by a factor of 4.

Figure 13 shows the measured transfer functions of the system without control and with the control applied, and the simulated transfer function of the controlled tube. The measured effects of the control of peaks 4 to 10 are detailed in Table IV. The damping factors obtained with the control have differences with the target values, with 10% to 35% error. The amplitude of all the peaks is reduced, with a maximum reduction for peak 7 with 10.3 dB. Apart from for the seventh peak, the increase in damping also has an effect on the peak frequency. Below the seventh peak, the frequency decreases (by as much as 53 cents for peak 4) while, above the seventh peak, the frequency increases (by

Document downloaded by @DAEL, 2026-11-21 15:19:12 - personal use only

Table IV. Modal parameters (frequency, amplitude, damping) of resonances 4 to 10 of the transfer functions (Figure 13) of the uncontrolled (U) and controlled (C) tubes, differences between intended (T) and obtained values for the frequencies and damping factors, and modifications obtained on the amplitudes.

Resonance		4	5	6	7	8	9	10
Frequency (Hz)	U	501	644	784	920	1050	1179	1311
	C	479	619	770	920	1063	1200	1357
	T	501	644	784	920	1050	1179	1311
Differences (cents)		53	48	22	0	15	21	42
Damping	U	0.0172	0.0141	0.0114	0.0113	0.0115	0.0100	0.0083
	C	0.0548	0.0481	0.0411	0.0343	0.0296	0.0267	0.0272
	T	0.0688	0.0564	0.0456	0.0452	0.0460	0.0400	0.0332
Differences (%)		20	15	10	24	35	33	18
Amplitude (dB)	U	-13.4	-11.3	-9.6	-8	-8.4	-10.5	-14.8
	C	-14.2	-17.1	-18.3	-18.3	-18.6	-18.8	-16.9
Modifications (dB)		-0.8	-5.8	-8.7	-10.3	-10.2	-8.3	-2.1

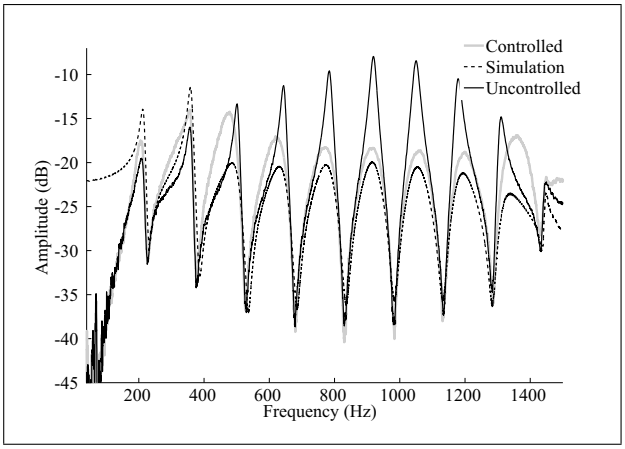


Figure 13. Measured transfer functions of the tube without control (solid black line) and with control of the damping of resonances 4 to 10, increased by a factor of 4 (solid gray line), and simulated transfer function of the controlled tube (dash black line).

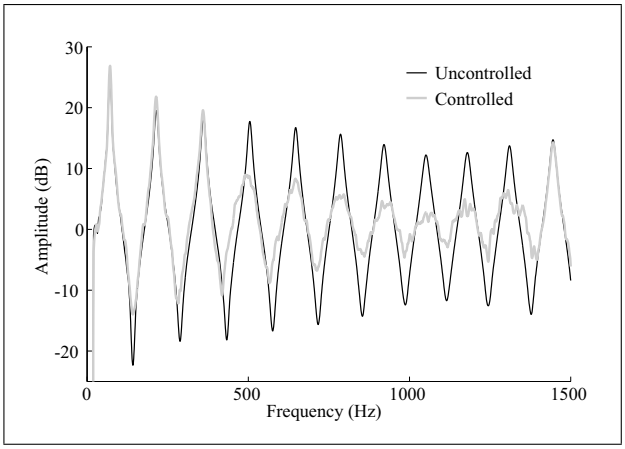


Figure 14. Input impedance magnitude of the tube without control (solid black line) and with control of the damping of resonances 4 to 10, increased by a factor of 4 (solid gray line).

as much as 42 cents for peak 10). The control also has an effect on the amplitudes of peaks 2 and 3, with respectively increases of 2.1 dB and 2 dB. Differences may be seen between the measured and simulated transfer functions of the tube, particularly with regard to the amplitude of the resonances (by as much as 6.5 dB difference on resonance 10). However, the amplitude of the resonances is modified in the same way, the amplitude of resonances 4 to 10 is reduced and the amplitude of the uncontrolled resonances 2 and 3 is increased. These differences may come from the simulation's speaker resonance (147.5 Hz), which is not modeled in matrix **A**, as evoked in Section 3.2. Mode 11 may be influenced by higher modes of the tube, which are not in the model.

Figure 14 shows the input impedance magnitude of the system without control and with the control applied. The effects of the control on peaks 4 to 10 are detailed in Table V. The amplitude of all the peaks is reduced, with a maximum reduction for peak 6 with 9.9 dB. Apart from for peaks 5 and 6, the increase in the damping also results in a decrease in the frequencies of the peaks, by as much as 29 cents for peak 4 (peak 5 is not modified and the frequency of peak 6 is increased). All the antiresonances are increased in amplitude by as much as 10 dB. The control also has an effect on the amplitudes of peaks 2 and 3, with respectively increases of 2.2 dB and 1.2 dB. These side effects may be due to the latency of the control setup, to calculation errors or to model errors.

Figure 15 shows the spectrogram of the sound emitted by the instrument, when blowing in it, with the control applied. In this figure, the control is applied between times 3 and 6 seconds. The control is applied while blowing in order to avoid reproductivity problems. With and without control, the pitch of the instrument corresponds to the first resonance of the tube. When the control is applied, odd harmonics 4 to 9 are weakened. Harmonic 10 is not shown on the figure, because it was too weak to be visible even before the control. The control also has an effect on the even harmonics, particularly on even harmonics 2 to 4 which are enhanced. This correlates with what has been

Document downloaded by @DAEL, 2026-11-21 15:19:12 - personal use only

Table V. Modal parameters of peaks 4 to 10 of the input impedance (Figure 14) of the uncontrolled (U) and controlled (C) tubes, differences between intended and obtained frequencies, and modifications obtained on the amplitudes.

Resonance		4	5	6	7	8	9	10
Frequency (Hz)	U	505	647	786	920	1052	1180	1310
	C	493	647	796	915	1050	1172	1307
Differences (cents)		29	0	15	7	2	8	3
Amplitude (dB)	U	17.7	16.7	15.7	14	12.2	12.6	13.7
	C	9	8.3	5.8	4.7	2.8	4.9	6.3
Modifications (dB)		-8.7	-8.4	-9.9	-9.3	-9.4	-7.7	-7.4

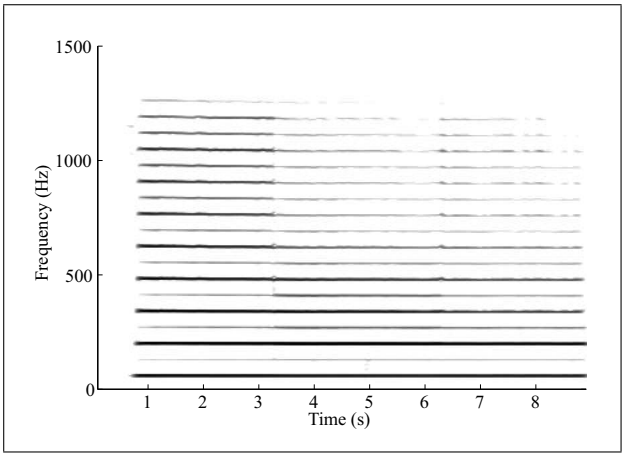


Figure 15. Spectrogram of the sound emitted by the instrument when increasing the damping of resonances 4 to 10 by a factor of 4. The control is applied for 3 seconds, between times 3 and 6 seconds.

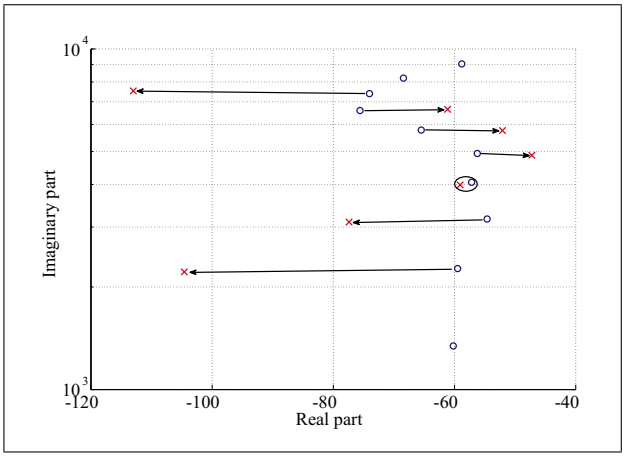


Figure 16. Pole placement for the poles of resonances 3 to 9 when controlling their frequencies and damping factors. Only the poles with positive imaginary values 2 to 11 are shown in a logarithmic scale.

observed on Figure 14. The next even harmonics are less enhanced than even harmonics 2 to 4 because they are less harmonically related to the fundamental of the sound. This control case is referred to as case **3** in Table IX.

3.4. Control of the damping and frequency of resonances 3 to 9

In Section 3.3, the control of the damping factor of seven resonances has been achieved. In this section, the damping factors and frequencies of resonances 3 to 9 are controlled. The frequencies of the resonances are chosen so that they are harmonically related to the frequency of the first peak of the input impedance (70.5 Hz). The damping factors are then chosen so that the peaks of the input impedance have minimum shift in amplitude.

Figure 16 shows the pole placement when applying the controls described in Table VI.

As the control does not move much the fifth pole, it is circled black in Figure 16.

Figure 17 shows the measured transfer functions of the system without control and with the control applied, and the simulated transfer function of the controlled tube.

The measured effects of the control on peaks 3 to 9 are detailed in Table VII (top). Differences with previous experiments come from different moment for the measurement (influence of the temperature on the frequency, etc.).

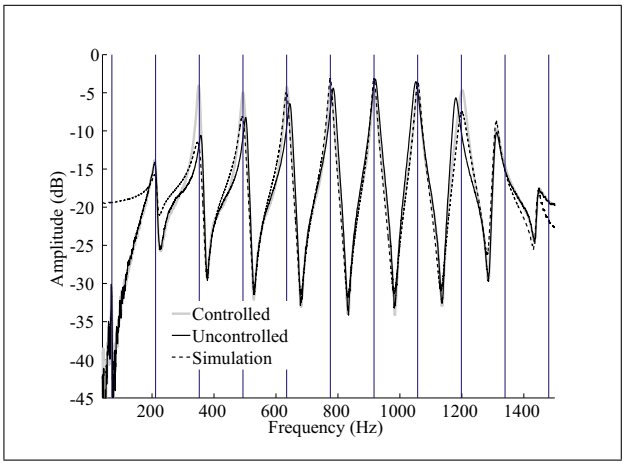


Figure 17. Measured transfer functions of the tube without control (solid black line) and with control of the frequencies and damping factors of resonances 3 to 9 (solid gray line), and simulated transfer function of the controlled tube (dash black line). The vertical lines show the odd harmonics of the first resonance.

The target frequencies for the resonances are close to the frequencies of the peaks, with no more than 7 cents difference for peak 3. As for the previous experiments, there are differences between obtained and targeted damping factors, with 1 % to 64 % error. The amplitude of peaks 3 to 6 and 9 increases with the control (by as much as

Document downloaded by @DAEL, 2026-11-21 15:19:12 - personal use only

Table VI. Targeted frequencies and damping factors change for resonances 3 to 9.

Resonance	3	4	5	6	7	8	9
Target frequency (Hz)	353	494	635	776	917	4058	1199
Target damping factor change	+80%	+45%	+5%	-15%	-20%	-20%	+50%

Table VII. Modal parameters (frequency, amplitude, damping) of resonances 3 to 9 of the transfer functions (Figure 17) of the uncontrolled (*U*) and controlled (*C*) tubes, differences between intended (*T*) and obtained values for the frequencies and damping factors, and modifications obtained on the amplitudes.

Resonance		3	4	5	6	7	8	9
Frequency (Hz)	*U*	358	503	645	785	921	1052	1181
	C	351	494	635	776	917	1057	1201
	T	353	494	635	776	917	1058	1199
Differences (cents)		7	0	0	0	0	1	2
Damping	*U*	0.0262	0.0172	0.0141	0.0114	0.0113	0.0115	0.0100
	C	0.0171	0.0155	0.0124	0.0100	0.0091	0.0080	0.0104
	T	0.0472	0.0249	0.0148	0.0097	0.0090	0.0092	0.0150
Differences (%)		64	38	16	3	1	13	31
Amplitude (dB)	*U*	-10.6	-8.3	-6.5	-4.4	-3.2	-3.5	-5.7
	C	-4.1	-5	-4.3	-4	-4.4	-4.1	-4.7
Modifications (dB)		+6.5	+3.3	+2.2	+0.4	-1.2	-0.6	+1

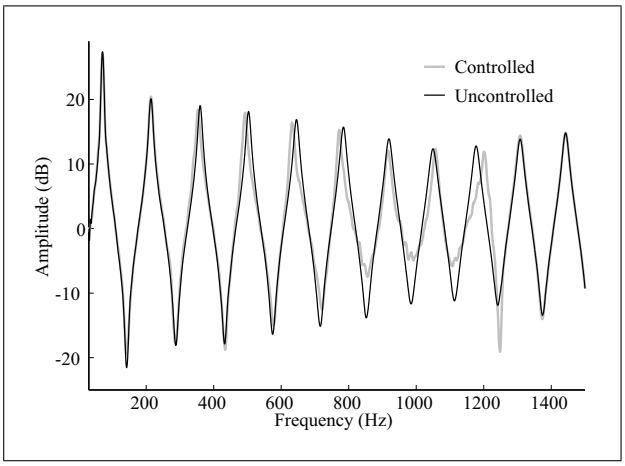


Figure 18. Input impedance magnitude of the tube without control (solid black line) and with control of the frequency and damping of resonances 3 to 9 (solid gray line).

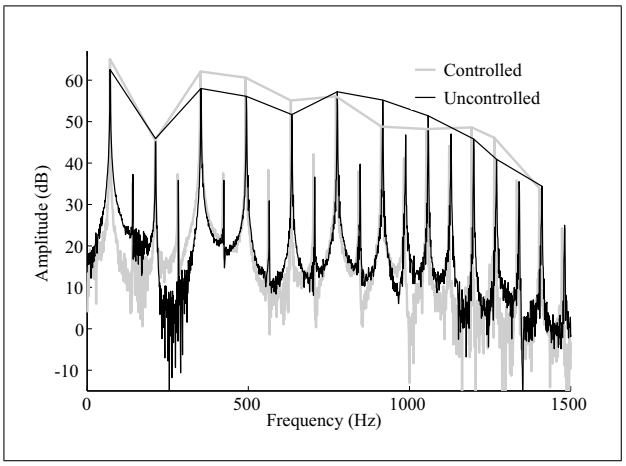


Figure 19. Enveloped sound spectra of the instrument when uncontrolled (solid black line) and when the frequencies and damping factors of resonances 3 to 9 are controlled (solid gray line).

6.5 dB for peak 3), while the amplitude of peaks 7 and 8 decreases with the control (by 1.2 dB and 0.6 dB respectively). The control has almost no effect on the other peaks. Simulated and measured transfer functions of the tube are close. However, differences may be seen between them, particularly with regard to the amplitude of resonances 3, 4 and 9 (by as much as 7.4 dB difference on resonance 3). The measured amplitude of these three resonances is higher than the simulated amplitude. The reasons of these differences are probably the same than evoked previously, that is the simulation's speaker resonance is not modeled, as well as modes higher than the eleventh.

Figure 18 shows the input impedance of the system without control and with the control applied. The effects of the control on peaks 3 to 9 are detailed in Table VIII. The frequencies of the peaks are close to the target of the control, with a maximum difference of 3Hz with peak 5 (difference of 6 cents). Apart from for peak 7, the amplitude is almost not modified (less than 1 dB), contrary to the transfer functions. The antiresonances between peaks 5 and 9 are increased in amplitude, by as much as 7 dB between peaks 7 and 8, while the antiresonance between peaks 9 and 10 is decreased in amplitude by 7.2 dB. There is almost no side effects of the control on the uncontrolled peaks.

The effect of the control cannot be easily seen on a spectrogram. To have a clearer view of the effect of the control, Figure 19 shows the sound spectra of the sound produced

Document downloaded by @DAEL, 2026-11-21 15:19:12 - personal use only

Table VIII. Modal parameters of peaks 3 to 9 of the input impedance (Figure 18) of the uncontrolled (U) and controlled (C) tubes, differences between intended and obtained frequencies, and modifications obtained on the amplitudes.

Resonance		3	4	5	6	7	8	9
Frequency (Hz)	U	360	504	646	785	920	1050	1175
	C	353	493	632	773	917	1057	1201
Differences (cents)		0	2	6	5	0	1	1
Amplitude (dB)	U	19	18.1	16.9	15.7	13.9	12.4	12.8
	C	18.4	18	16.4	15.3	12.1	12.3	11.9
Modifications (dB)		-0.6	-0.1	-0.5	-0.4	-1.8	-0.1	-0.9

by the instrument without control and with the control applied. With and without control, the pitch of the instrument corresponds to the first resonance of the tube, but it appears that the pitch of the sound is modified, from 70.6 Hz without control to 70.2 Hz with the control applied, that is a difference of 7 cents. There also are modifications of the amplitude of the harmonics. Between 0 and 750 Hz and between 1100 Hz and 1400 Hz, the amplitude of the harmonics of the sound produced by the controlled instrument are higher, by as much as 4 dB at 352 Hz and 5 dB at 1263 Hz. Between 750 Hz and 1100 Hz, the amplitude of the harmonics of the sound produced by the controlled instrument are weaker, by as much as 6 dB at 917 Hz. The increases of amplitude may be due to the fact that the resonances are better harmonically related with the first peak of the input impedance. The decrease of amplitude around the seventh resonance corresponds to the only peak which is weaker in the input impedance when controlled. This control case is referred to as case **4** in Table IX.

3.5. Radiated Sound Characterisation

In this section, a comparison is made between the sound radiated by the instrument when uncontrolled and controlled in three cases of control:

- the control of f_7 of Section 3.2, referred to as case **1**,
- the control of ξ_{4-10} of Section 3.3, referred to as case **3**,
- the control of resonances 3 to 9 of Section 3.4, referred to as case **4**.

The control of ξ_7 of Section 3.2 is not used in this Section, as the *slap* sounds have been produced during different blows. Moreover, applying the control while blowing in this case does not have noticeable effects.

The comparisons between sounds, measured one meter away from the output of the instrument, are done using three criteria:

- the sound level,
- the spectral centroid, which is connected to the "brilliance" of the sound [31],
- the pitch.

The sound level L is calculated with

$$L_{dB_{SPL}} = 10 \log_{10} \left(\frac{p^2}{p_0^2} \right), \tag{12}$$

Table IX. Differences of sound level, spectral centroid and pitch of the radiated sound between uncontrolled and controlled instrument in three cases of control.

Control cases	1	3	4
Sound level (dB_{SPL})	-0.91	-2.02	+0.25
Spectral Centroid (Cents)	-8	-107	-205
Pitch (Cents)	-3	-7	-7

where p is the measured pressure signal, and p_0 the reference value. As the comparison is done between uncontrolled and controlled instruments, p_0 is the mean value of the RMS pressure amplitude during time without applying the control, and p is the mean value of the RMS pressure amplitude during time when the instrument is controlled.

The frequency of the spectral centroid f_{sc} is calculated using [32]

$$f_{sc} = \frac{\sum_{f=1}^{f=N} f x(f)}{\sum_{f=1}^{f=N} x(f)}, \tag{13}$$

where f is the frequency, N half the sampling frequency of the measured signal (here, $N = 22050$ Hz) and $x(f)$ the amplitude of the spectrum of the sound at frequency f.

Table IX presents these differences. The sound level is reduced in cases **1** and **3**. In case **1**, this may be due to decrease of the amplitude of high harmonics in the sound when f_7 is moved. In case **3**, this is due to the increase of the damping of the resonances. As most of the harmonics with frequencies higher than the frequency of the fourth harmonic are no longer audible, the sound is lower. There is almost no modification of the sound level in case **4**.

The differences of spectral centroids are shown in cents because it has a different value, regarding to the way the instrumentalist blows in the instrument. If the musician blows harder, the high frequency harmonics in the sound are enhanced, then the spectral centroid is higher in frequency. In case **1**, it is close to 300 Hz, which correlates with Sandell [32]. In cases **3** and **4**, it is close to 600 Hz. In every cases of control, the spectral centroid is lower in frequency, which indicates a "darker" sound, particularly with control case **4**. It seems that the more the control is complex, the more the spectral centroid moves toward the low frequencies.

In every cases, the pitch is a bit lower when the control is applied.

Document downloaded by @DAEL, 2026-11-21 15:19:12 - personal use only

4. Conclusion and Perspectives

In this paper, an experimental validation of modal active control using a pole placement algorithm applied to a simplified self-sustained musical wind instrument in order to modify its emitted sound has been presented. To the authors' knowledge, it is the first time that such a control has been applied to a self-sustained system. The effects of this control have been studied with four sets of measurements. Modifications were observed of:

- the peaks of the transfer functions,
- the peaks of the input impedance,
- the sound level of the instrument under playing condition,
- the strength of the harmonics in the sound emitted when the instrument is blown and, consequently, the "brilliance" of the sound,
- the duration of the harmonics in the sound emitted by the instrument when blowing ceases,
- the pitch of the sound emitted by the instrument.

The controller has been shown to be very accurate with respect to the control of the frequencies of the resonances, although the control of their damping factors was not as precise. Sometimes the control led to unintended modifications of the amplitudes of the uncontrolled resonances. This may be due to the latency of the control setup, to calculation errors or to modelling errors. When the control is applied to seven modes, differences have been observed between the measured mode amplitudes and those predicted by simulations. This is probably due to the absence of the first resonance in the model as well as modes higher than the eleventh. However, these differences do not lead to instabilities. Meanwhile, the control of the resonances has been shown to lead to modifications in the spectrogram of the sounds produced by the simplified clarinet. The harmonics in the sound were observed to be weakened as a result of either the control changing the resonance frequencies and reducing their harmonicity, or as a result of the control increasing the damping of the resonances. Conversely, the harmonics were observed to be strengthened as a result of the control changing the resonance frequencies and increasing their harmonicity, or as a result of the control decreasing the damping of the resonances. The effects are similar to what would happen with modifications of the bore profile of the instrument.

Although these experiments have demonstrated the great potential of modal active control for modifying the frequencies and damping factors of the resonances of a wind instrument, it should be noted that the current controller cannot modify the first and second resonances of the system. This is due to both how it is positioned within the tube and the components from which it is made up. In future, by using other control devices, such as piezoelectric rings or films embedded within the wall of the tube (without modifying its internal structure), it may be possible to control these two resonances. Even with such a change in hardware, the control method described in this paper is not able to modify the amplitude of the resonances without altering their damping or frequencies. However, a combined state and derivative state control of the system may in future enable this to be achieved [18, 33].

It is next planned to apply modal active control to real musical wind instruments, starting with a bass clarinet.

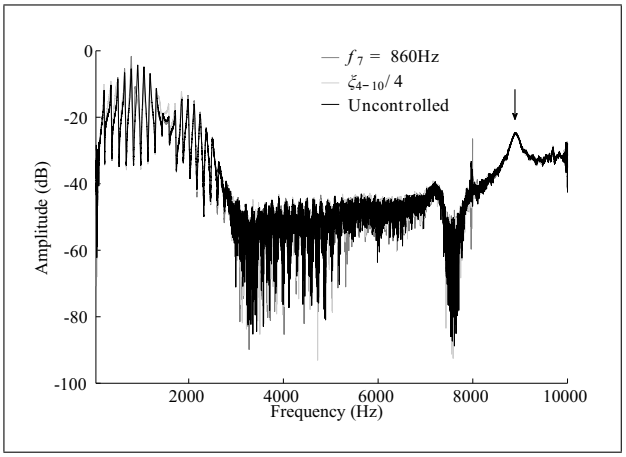


Figure A1. Transfer functions of the tube without control (solid black line), with control of the frequency of the seventh resonance (solid dark grey line) and with control of the damping factors of resonances 4 to 10 (solid light gray line). The arrow points out the first mode transverse to the tube.

Appendix: Transversal modes

When modal active control is applied to a system, instabilities may happen with the unmodeled modes of the system. This phenomenon is called spillover [1]. The control system of the simplified bass clarinet is co-located, it is then possible to obtain instabilities on the modes transverse to the tube. Figure 20 presents the transfer functions of the instrument, measured between the speaker and microphone of the control system, without control and with the control of the seventh resonance frequency of Section 3.2, and with the control of the damping of resonances 4 to 10 of Section 3.3. These transfer functions are studied up to 10000 Hz so that the first mode transverse to the tube may be observed. It is indicated with an arrow in Figure 20, and it has a frequency of 8994 Hz. This resonance is not modified when the control is applied, and the system is not unstable due to this resonance. There is no spillover due to these modes.

Acknowledgements

This work was carried out during the PhDs of Simon Benacchio and Thibaut Meurisse, funded by Agence Nationale de la Recherche (ANR IMAREV project) and Université Pierre et Marie Curie (UPMC, Paris 6). We thank gratefully Robert Piéchaud for his help with Xenomai, and Alain Terrier for his precious help in building the system. We thank the Newton International Fellowship scheme for funding the collaboration between France and UK.

Document downloaded by @DAEL, 2026-11-21 15:19:12 - personal use only

References

[1] C. R. Fuller, S. J. Elliott, P. A. Nelson: Active Control of Vibration. Academic Press, 1996.

[2] R. T. Schumacher: Self-Sustained Oscillations of the Clarinet: An Integral Equation Approach. Acustica **40** (1978) 298–309.

[3] M. E. McIntyre, R. T. Schumacher, J. Woodhouse: On the oscillations of musical instruments. J. Acoust. Soc. Am. **74** (1983) 1325-.1345.

[4] A. Hirschberg: Aero-Acoustics of Wind Instruments. In: G. Weinreich, A. Hirschberg, J. Kergomard (eds.): Mechanics of Musical Instruments. Volume 335 of CISM Courses and Lectures. Springer-Verlag, Wien - New York, 1995, 291–369.

[5] F. Silva, J. Kergomard, C. Vergez, J. Gilbert: Interaction of reed and acoustic resonator in clarinetlike systems. J. Acoust. Soc. Am. **124** (2008) 3284–3295.

[6] S. Karkar, C. Vergez, B. Cochelin: Toward the systematic investigation of periodic solutions in single reed woodwind instruments. Proc. of the 20th Int. Symp. on Music Acoustics, Associated Meeting of the International Congress on Acoustics, International Commission for Acoustics, Sydney, Australia, 2010, 1–7.

[7] S. Karkar, C. Vergez, B. Cochelin: Oscillation threshold of a clarinet model: A numerical continuation approach. J. Acoust. Soc. Am. **131** (2012) 698–707.

[8] C. Besnainou: Modal Stimulation: a Sound Synthesis New Approach. Proc. of the Int. Symp. on Music Acoustics 1995, Dourdan, France, 1995. 434–438.

[9] H. Boutin: Méthodes de contrôle actif d'instruments de musique. Cas de la lame de xylophone et du violon. (Musical instruments active control methods. Cases of the xylophone bar and of the violin.) Phd Thesis, Université Pierre et Marie Curie - Paris VI, 2011.

[10] E. Berdahl, J. Smith: Feedback control of acoustic musical instruments: Collocated control using physical analogs. J. Acoust. Soc. Am. **131** (2012) 963–973.

[11] J. Guérard: Modélisation numérique et simulation expérimentale de systèmes acoustiques - Application aux instruments de musique. (Digital modeling and experimental simulation of acoustical systems - Application to musical instruments.) Phd Thesis, Université Pierre et Marie Curie - Paris VI, 2002.

[12] A. Mamou-Mani, T. Meurisse, B. Sluchin, R. Caussé: La sourdine active: effets sur les premières résonances du trombone. Proc. 12th Congrès Francais d'Acoustique (CFA 2014), Poitiers, France. 22–25 april 2014, 1583-1586.

[13] T. Meurisse, A. Mamou-Mani, R. Caussé, D. Sharp: Active control applied to simplified wind musical instrument Proc. Int. Cong. on Acoustics 2013, Montréal, Canada. 2.-7 June 2013, Vol.19, 2pEAb7.

[14] J. Hong *et al.*: Modeling, Identification, and Feedback Control of Noise in an Acoustic Duct. IEEE Transactions on Control Systems Technology **4** (1996)

[15] B. Chomette, D. Remond, S. Chesné, L. Gaudiller: Semi-adaptive modal control of on-board electronic boards using identication method. Smart Material and Structures **17** 2008 1–8.

[16] T. Meurisse, A. Mamour-Mani, R. Caussé, B. Chomette, D. Sharp: Simulations of Modal Active Control Applied to the Self-Sustained Oscillations of the Clarinet Acta Acustica united with Acustica **100** (2014) 1149–1161.

[17] S. Hanagud, S. Griffin: Active Structural Control for a Smart Guitar. Proc. 4th European Conference On Smart Structures and Materials, Harrogate, United Kingdom. July 6–8 1998.

[18] S. Benacchio, A. Mamou-Mani, B. Chomette, F. Ollivier: Simulated Effects of Combined Control Applied to an Experimentally Identified Soundboard. Proc. of the Stockholm Music Acoustics Conference 2013 (SMAC 2013), Stockholm, Sweden. August 2013.

[19] M. Campbell: Objective evaluation of musical instrument quality: A grand challenge in musical acoustics. Proc. of Meetings on Acoustics **19**, 2 June 2013.

[20] E. Poirson, P. Depince, J. F. Petiot: User-centred design by genetic algorithms: Application to brass musical instrument optimization. Eng. Appl. Artif. Intel. **20** (2007) 511–518.

[21] P. Eveno, J. F. Petiot, J. Gilbert, B. Kieffer, R. Caussé: The relationship between bore resonance frequencies and playing frequencies in trumpets. Acta Acustica united with Acustica **100** (2014) 362–374.

[22] N. H. Fletcher, T. D. Rossing: The Physics of Musical Instruments. Springer-Verlag, New York, 1991.

[23] A. Mamou-Mani, D. Sharp, T. Meurisse, W. Ring: Investigating the consistency of woodwind instrument manufacturing by comparing five nominally identical oboes. J. Acoust. Soc. Amer. **131** (2012) 728–736.

[24] T. Richardson, D. Formenti: Parameter estimation from frequency response measurements using rational fraction polynomials. 1eIMAC Conference, 1982.

[25] D. Luenberger: An introduction to Observers. IEEE Transactions on Automatic Control **16** (1971) 596–602.

[26] A.Preumont: Vibration Control of Active Structures, An Introduction - Third Edition. Springer, 2011, p.197.

[27] J. Kautsky, N. K. Nichols: Robust Pole Assignment in Linear State Feedback. Int. J. Control **41** (1985) 1129–1155.

[28] http://www.xenomai.org/

[29] C. Blaess: Solutions temps réel sous Linux. Eyrolles, 2012.

[30] S. Benacchio, R. Piéchaud, A. Mamou-Mani, B. Chomette, V. Finel: Active Control of String Instruments using Xenomai. Proc. Fifteenth real-Time Linux Workshop, Lugano-Manno, Switzerland. October 28-31 2013, 133–141.

[31] J. M. Grey, J. W. Gordon: Perceptual effects of spectral modifictions on musical timbres. J. Acoust. Soc. Am. **63** (1978) 1493.

[32] G. J. Sandell: A Library of Orchestral Instrument Spectra. ICMC International Computer Music Conference, Montreal. 16-20 October 1991.

[33] S. Benacchio, A. Mamou-Mani, B. Chomette, F. Ollivier: Combined State and State Derivative Control Applied to Musical String Instruments. Proc. Int. Cong. on Acoustics 2013, Montréal, Canada. 2–7 June 2013, Vol.19, 4pSA3.

Document downloaded by @DAEL, 2026-11-21 15:19:12 - personal use only